Plasmonic chiral contrast agents for optical coherence tomography: numerical study

Kalpesh B. Mehta[1,2,*] and Nanguang Chen[1,2]

[1]*Optical Bioimaging Lab, Division of Bioengineering, National University of Singapore, 7 Engineering Drive 1, Blk E3A, 04-15, Singapore 117574, Singapore*

[2]*NUS Graduate School of Integrative Sciences and Engineering, National University of Singapore, Singapore 117456, Singapore*

**kalpesh@nus.edu.sg*

Abstract: Optical coherence tomography (OCT) is a widely used morphological imaging modality. Various contrast agents, which change localized optical properties, are used to extend the applicability of OCT, where intrinsic contrast is not sufficient. In this paper we propose the use of a dual-rod gold nano-structure as a polarization sensitive contrast agent. Using numerical simulation, we demonstrated that the proposed structure has tunable chiral response. Enhanced cross-section due to Plasmon resonance in gold nanoparticles, along with the chiral behavior can provide enhanced detection sensitivity. The proposed contrast agents may extend the applicability of OCT to the problems that require the molecular contrast with enhanced sensitivity.

OCIS codes: (290.5855) Scattering, polarization; (170.4500) Optical coherence tomography; (110.0113) Imaging through turbid media; (160.1585) Chiral media.

References and links

1. S. A. Boppart, A. L. Oldenburg, C. Xu, and D. L. Marks, "Optical probes and techniques for molecular contrast enhancement in coherence imaging," J. Biomed. Opt. **10**(4), 041208 (2005).
2. P. K. Jain, K. S. Lee, I. H. El-Sayed, and M. A. El-Sayed, "Calculated absorption and scattering properties of gold nanoparticles of different size, shape, and composition: applications in biological imaging and biomedicine," J. Phys. Chem. B **110**(14), 7238–7248 (2006).
3. S. J. Oldenburg, R. D. Averitt, S. L. Westcott, and N. J. Halas, "Nanoengineering of optical resonances," Chem. Phys. Lett. **288**(2-4), 243–247 (1998).
4. Y. Sun and Y. Xia, "Gold and silver nanoparticles: a class of chromophores with colors tunable in the range from 400 to 750 nm," Analyst (Lond.) **128**(6), 686–691 (2003).
5. C. Loo, A. Lin, L. Hirsch, M. H. Lee, J. Barton, N. Halas, J. West, and R. Drezek, "Nanoshell-enabled photonics-based imaging and therapy of cancer," Technol. Cancer Res. Treat. **3**(1), 33–40 (2004).
6. S. E. Skrabalak, L. Au, X. Lu, X. Li, and Y. Xia, "Gold nanocages for cancer detection and treatment," Nanomedicine (Lond) **2**(5), 657–668 (2007).
7. T. S. Troutman, J. K. Barton, and M. Romanowski, "Optical coherence tomography with plasmon resonant nanorods of gold," Opt. Lett. **32**(11), 1438–1440 (2007).
8. C. L. Nehl, H. Liao, and J. H. Hafner, "Optical properties of star-shaped gold nanoparticles," Nano Lett. **6**(4), 683–688 (2006).
9. J. Aaron, E. de la Rosa, K. Travis, N. Harrison, J. Burt, M. José-Yacamán, and K. Sokolov, "Polarization microscopy with stellated gold nanoparticles for robust monitoring of molecular assemblies and single biomolecules," Opt. Express **16**(3), 2153–2167 (2008).
10. A. F. Fercher, W. Drexler, C. K. Hitzenberger, and T. Lasser, "Optical coherence tomography - principles and applications," Rep. Prog. Phys. **66**(2), 239–303 (2003).
11. V. Tuchin, L. Wang, and D. Zimnyakov, "Tissue structure and optical models," in *Optical Polarization in Biomedical Applications* (Springer, 2006), pp. 7–28.
12. C. Bustamante, M. F. Maestre, and J. Tinoco, "Circular intensity differential scattering of light by helical structures. I. Theory," J. Chem. Phys. **73**(9), 4273–4281 (1980).
13. A. Y. Elezzabi and S. Sederberg, "Chirality and optical activity: a terahertz time-domain spectroscopy investigation," Proc. SPIE **7214**, 72140O (2009).
14. Y. Svirko, N. Zheludev, and M. Osipov, "Layered chiral metallic microstructures with inductive coupling," Appl. Phys. Lett. **78**(4), 498–500 (2001).
15. E. Plum, V. A. Fedotov, A. S. Schwanecke, N. I. Zheludev, and Y. Chen, "Giant optical gyrotropy due to electromagnetic coupling," Appl. Phys. Lett. **90**(22), 223113 (2007).

#145356 - $15.00 USD Received 4 Apr 2011; revised 20 May 2011; accepted 2 Jun 2011; published 19 Jul 2011

16. A. Taflove and S. C. Hagness, *Computational Electrodynamics: The Finite-Difference Time-Domain Method*, 3rd ed. (Artech House Publishers, 2005).
17. Lumerical Solutions Inc, FDTD Solutions. 2010, http://www.lumerical.com/fdtd.php.
18. S. J. Orfanidis, *Electromagnetic Waves and Antennas* (2010), http://www.ece.rutgers.edu/~orfanidi/ewa/.
19. "IEEE standard definitions of terms for antennas," IEEE Trans. Antenn. Propag., AP-31 (1983).
20. M. C. Pierce, J. Strasswimmer, B. Hyle Park, B. Cense, and J. F. De Boer, "Birefringence measurements in human skin using polarization-sensitive optical coherence tomography," J. Biomed. Opt. **9**(2), 287–291 (2004).
21. P. J. Holmes and J. E. Snell, "A vapour etching technique for the photolithography of silicon dioxide," Microelectron. Reliab. **5**(4), 337–341 (1966).

1. Introduction

In optical imaging methods, various extrinsic agents are used to enhance contrast and to improve signal to noise ratio. The enhanced contrast can be used to detect molecules or various biological entities, which do not provide sufficient intrinsic contrast. With enhanced contrast, imaging methods can be used to provide better understanding of biological processes or enhanced detection capability for diseases [1]. The contrast agents introduce localized mismatch in optical properties to provide unique optical signature that can be easily detected by optical imaging methods.

Several agents have been designed and used for coherence-based imaging methods [1]. Metallic nanoparticles are widely used as agents for coherence imaging methods as they provide several advantages: high scattering, high absorption cross section due to the Plasmon resonance phenomenon, tunable resonance wavelength, inertness (of gold and silver) in biological tissues [2]. The resonance wavelength can be tuned by controlling the size and shape of the structure, and composition of the particles [3,4]. Gold and silver nanoparticles of various shapes, sizes and compositions have been designed and used for various bioimaging applications [5–7]. In these applications, imaging methods have been used to detect the enhancement in scattering/absorption cross section as an optical signature that improves contrast.

Apart from enhancement in the scattering/absorption cross section, properly designed nanoparticles along with a suitable imaging method can provide more efficient background rejection leading to better signal to noise ratio and better contrast. For example: one can exploit nanostructures that are sensitive to polarization of the illumination to further enhance the contrast [8,9]. In the coherence imaging systems with linearly polarized incident light, it has been demonstrated that symmetrical particles do not depolarize incident light. To improve contrast, asymmetrical stellated nanoparticles have been fabricated to provide increased depolarized scattered light for linearly polarized incident light. Improvement in the detection sensitivity has been achieved by using them in dark-field polarization sensitive microscopes [9].

Due to high imaging depth, good resolution and possibility of obtaining in-vivo images, Optical coherence tomography (OCT) has been used in many biological applications [10]. OCT is essentially a morphological imaging modality that detects the backscattered light and has no molecular specificity. Gold nanoparticles, conjugated to various biomolecules, have been used with OCT to visualize the molecular concentration in thick biological tissues. However, the scattering signal from nanoparticles may not be easily distinguishable from the background signal due to other microscopic scatterers in tissue, thus limiting the detection sensitivity.

In coherence imaging, a few biological structures (such as collagen) provide polarization dependent response [11]. However, it is rare to find biological entities with significant chiral behavior at optical wavelengths. Unlike normal materials, chiral materials differentially scatter the left-circularly and the right-circularly polarized light [12,13]. By injecting chiral contrast agents in a tissue and imaging with a circular polarization sensitive coherence imaging method (that differentiates the highly-chiral response of the contrast agent from the non-chiral or less-chiral response from the surrounding tissue), a significant improvement in signal to noise ratio and detection sensitivity may be achieved.

Previous research has demonstrated that microscopic bilayer metallic pattern has chiral response to normally incident light as it provides optical rotation to linearly polarized

#145356 - $15.00 USD Received 4 Apr 2011; revised 20 May 2011; accepted 2 Jun 2011; published 19 Jul 2011

normally incident light [14,15]. In this paper, we propose use of a chiral dual rod gold nanoparticles as contrast agents to improve signal to noise ratio in biological specimens. We demonstrate that the proposed nanoparticles provide differential response to left circularly polarized (LCP) and right circularly polarized (RCP) incident light, as well as enhanced scattering cross section due to Plasmon resonance. Numerical simulations based on the Finite Difference Time Domain (FDTD) method [16] have been used to characterize the particles and demonstrate the polarization dependent behavior and enhanced scattering cross-sections. We have provided designs for the particles with resonance at 800 nm and 1310 nm. To enable detection of the circular polarization dependent behavior of nanoparticles, we describe simple modifications required in the conventional OCT system.

Due to enhancement in scattering due to Plasmon resonance, circular polarization dependent optical response of the proposed particles can be readily differentiated from the background using proposed modifications of the OCT system. Thus, proposed nanoparticles can be used to image molecular information with improved sensitivity using OCT.

2. 3-D chiral particle and simulation method

A simple dual rod chiral nanoparticle considered in our study is shown in Fig. 1. The particle consists of two metallic rods patterned on a dielectric layer. As it is possible to achieve desired resonance wavelengths (e.g., 800nm, 1310nm) using gold and silicon nitride is a standard dielectric material used in the semiconductor fabrication process, we have chosen gold and silicon nitride in this study. The resonance wavelength of the particle depends on the dimensions of the gold nanobars, properties of the dielectric material, and spacing between both bars.

The chiral behavior of the particle is due to the relative angle (θ_r) and the distance (D) between gold nanobars. Parameters D and θ_r affect the manner in which the nanoparticles interact with different polarization states of the incident light. To define the angle θ_r, consider the particle orientation as shown in the Fig. 1. The incident light propagates in the $\hat{z}$ direction, the first gold nanobar (the bottom layer) has its major axis oriented along $\hat{l}_b$, and second gold nanobar (the top layer) has its major axis oriented along $\hat{l}_t$ as shown in Fig. 1. The angle θ_r is measured from $\hat{l}_b$ to $\hat{l}_t$ in the clockwise direction.

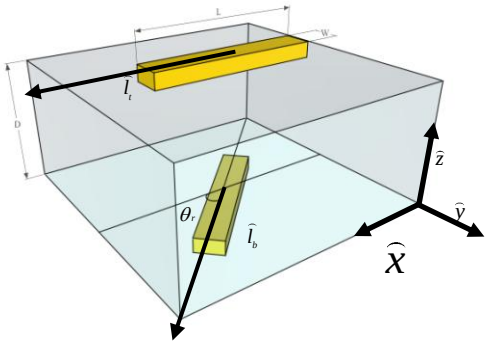

Fig. 1. A Three dimensional chiral structure, Dimensions of gold nanorods (L,W) determines resonance wavelength, D and θ_r controls chirality.

We have used the Finite Difference Time Domain (FDTD) method to numerically investigate the behavior of the particle. Such an analysis provides a valuable assessment of the scattering properties of the proposed particles and establishes important design parameters, which are prerequisite to the fabrication and use of such particles as contrast agents. A commercial software, LUMERICAL [17], is used to carry out simulations. To characterize the

#145356 - $15.00 USD Received 4 Apr 2011; revised 20 May 2011; accepted 2 Jun 2011; published 19 Jul 2011

scattering properties of the particle, a finite simulation region with a particle and surrounding medium of water is used. As the scattering problem is intrinsically an open-boundary problem, proper truncation boundary conditions are necessary to make simulation region finite. It is also necessary to have boundary conditions which do not cause spurious reflections due to impedance mismatch [16], otherwise the spurious response can lead to erroneous results. Perfectly matched layers (that match the impedance at the edges of the simulation region and provide attenuation to field) are designed, so that we can characterize a particle as if it is in the free space [16] using a finite simulation geometry. Far-field scattered electric field in the backscattered region is calculated for two orthogonal linearly polarized incident plane waves. LUMERICAL allows scattering analysis for only linearly polarized light. To obtain response of the particles to the LCP light and RCP light, we use the fact that LCP and RCP are superposition of the two orthogonal linearly polarized components [18]. We calculate the response for two linearly polarized orthogonal sources and properly superpose the complex field responses to obtain the scattered field values for LCP and RCP. Throughout the paper IEEE convention has been used to define LCP and RCP waves [19].

To quantify differential response to LCP and RCP incident light, we introduce a parameter termed Circular intensity differential scattering (CIDS). These parameters are calculated using the field values obtained by FDTD. CIDS is defined as:

$$CIDS(\omega) = \frac{I_{LCP}(\omega) - I_{RCP}(\omega)}{I_{LCP}(\omega) + I_{RCP}(\omega)} \tag{1}$$

where, intensity $I(\omega)$ is calculated using the Eq. (2), which takes numerical aperture of the optical setup into the account.

$$I(\omega) = \left| \int_{\phi=0}^{2\pi} \int_{\theta=180-\frac{\alpha}{2}}^{180+\frac{\alpha}{2}} \vec{E}(\omega,\theta,\phi)\sin(\theta)\,d\phi\,d\theta \right|^2 \tag{2}$$

where, $\vec{E}(\omega,\theta,\phi)$ is the back-scattered field obtained using the FDTD simulations, numerical aperture $NA = n\sin(\alpha)$. I_{LCP} is the total backscattered field intensity for the left-hand circularly polarized (LCP) incident light and I_{RCP} is the total backscattered field intensity for the right-hand circularly polarized (RCP) incident light for the angular frequency ω of the incident light.

CIDS and back reflected intensity obtained by Eq. (1) and Eq. (2) are monochromatic parameters, which we calculated for a range of wavelengths. OCT uses broadband source to obtain depth-dependent reflectivity. The depth-dependent reflectivity is proportional to the integral over source frequencies of the product of the power spectral density of the source and backscattered intensity calculated in Eq. (2) [10].

$$R \propto \int_{\omega} \left[\int_{\phi=0}^{2\pi} \int_{\theta=180-\frac{\alpha}{2}}^{180+\frac{\alpha}{2}} I(\omega,\theta,\phi)\sin(\theta)\,d\phi\,d\theta \right] .PSD(\omega)\,d\omega \tag{3}$$

where, R is the depth dependent reflectivity and PSD is the power spectral density of the source. Normalized difference in reflectivity (Eq. (4)) is used to quantify differential response of nanoparticles that can be observed by the proposed OCT system. In our study, we have used broadband sources with the center wavelength of 800nm, 1310 nm, and bandwidth of 75nm, 150nm respectively.

The normalized difference in the reflectivity (ΔR) is defined as,

#145356 - $15.00 USD Received 4 Apr 2011; revised 20 May 2011; accepted 2 Jun 2011; published 19 Jul 2011

$$\Delta R = \frac{R_L - R_R}{R_L + R_R} \tag{4}$$

R_L is the reflectivity of the particle for left circularly polarized incident light and R_R is the reflectivity of the particle for right circularly polarized incident light for the broadband source.

To demonstrate the enhancement in the scattering due to Plasmon resonance, we have also calculated the differential backscattering cross section (DSC) for both RCP and LCP incident lights. Note that the term 'differential' in DSC (a standard parameter used in antenna design) implies computation of cross-section over a finite numerical aperture.

$$\sigma_{dsc}(\omega) = \frac{\int_{\phi=0}^{2\pi} \int_{\theta=180-\frac{\alpha}{2}}^{180+\frac{\alpha}{2}} P_{backscatterd}(\omega,\theta,\phi)\sin(\theta)\,d\phi\,d\theta}{I_{inc}(\omega)} \tag{5}$$

where, $P_{backscatterd}$ is the back scattered power from the particle (Watt) and I_{inc} is the incident power density (Watt/m^2). DSC is useful to determine the strength of the back-scattered signal, whereas CIDS and normalized difference in reflectivity are parameters that quantify the differential response to sense of the circularly polarized light. To obtain good signal to background (with respect to the endogenous scattering entities) ratio, high CIDS and normalized difference in reflectivity are required. For achieving good signal to noise ratio, high values of DSC are required.

3. Results and discussion

It is possible to tune the resonance wavelength by changing the dimensions of the nanorods in the particle. We present the differential scattering cross section of the particle for two sets of dimensions. The dimensions were selected such that the structures resonate at around 800nm and 1310 nm [Fig. 2], widely used wavelengths for OCT [10]. For the simulations, we considered a single chiral particle oriented such that the long axis of gold nanobars are perpendicular to the propagation direction of the incident light.

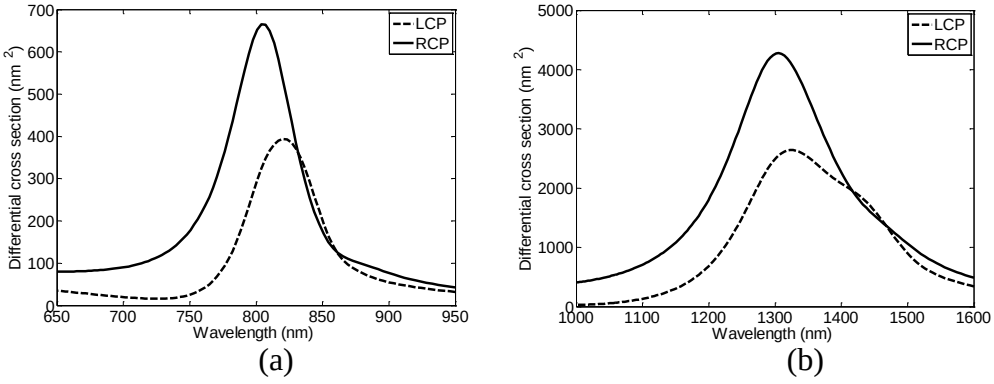

Fig. 2. Differential Scattering Cross section for the particle for LCP and RCP incident lights for single particle Dimensions of the particle used in the simulation are: (a) L = 70 nm, W = 30 nm, D = 68 nm, θ_r = 45° (b) L = 175 nm, W = 30 nm, D = 81 nm, θ_r = 45°, NA = 0.35.

From the Fig. 2, it is evident that when the particles are oriented normally to the incident light direction, they provide scattering dependent on the polarization of the incident light. Next, we demonstrate that even the average scattering for all possible orientations of the nanoparticles provides similar polarization dependent chiral behavior. In 3-D space, distinct

#145356 - $15.00 USD Received 4 Apr 2011; revised 20 May 2011; accepted 2 Jun 2011; published 19 Jul 2011

orientations of a particle can be obtained by an azimuth rotation (φ) followed by the polar (θ) rotation with respect to its starting position. In the simulations, we have used circularly polarized incident light propagating along $\hat{z}$. An azimuthal rotation is equivalent to rotating the incident light field azimuthally, leading to phase change only for the circularly polarized incident light. Due to the inherent symmetry of the imaging system, the particle displays azimuth (φ) rotation independent response. On the other hand, particle will have distinct response for different polar rotational angles. We compute the particle's response for different polar orientations of the particle, which were obtained by rotating the particle by polar angle (θ) values 0^o to 180^o in steps of 5^o .

If the particles are injected in the biological specimen, particles will have random orientations and locations. Thus, obtaining their collective optical response requires that we compute average intensity of the backscattered light from different particles. Figure 3 shows the intensity averaged over all particle orientations, and CIDS calculated from the averaged intensities.

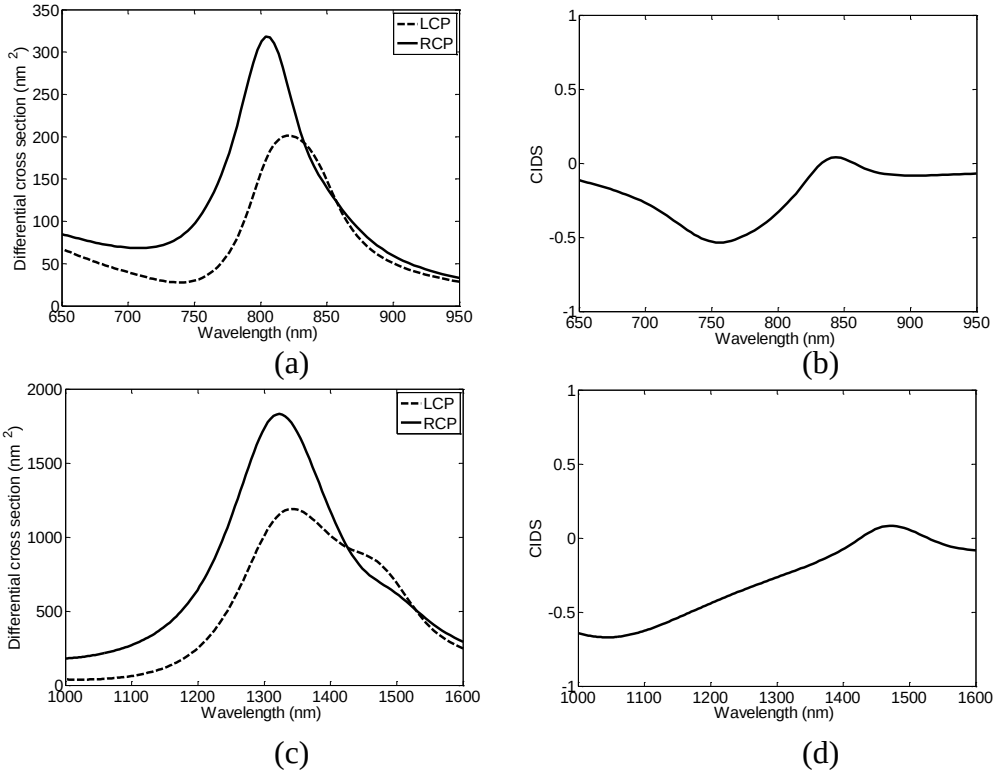

Fig. 3. (a), (c) Averaged differential scattering cross section obtained by rotating the particles at finite steps (0^0 to 180^o) (b), (d) CIDS calculated using the averaged backscattered field intensities for LCP and RCP lights. Dimensions for (a) and (b): L = 70 nm, W = 30 nm, D = 68 nm, θ_r = 45°, Dimensions for (c) and (d): L = 175 nm, W = 30 nm, D = 81 nm, θ_r = 45°, NA = 0.35.

It is evident that even in the case of random orientations, these particles still show a net polarization dependent behavior. Around the resonance wavelength, we observe $30-40\%$ difference in the backscattered intensities for LCP and RCP incident light.

We also computed the normalized difference in reflectivity. We assumed Gaussian power spectral density of the source, center wavelengths to be 800 nm and 1310 nm, and bandwidths to be 75nm and 150 nm, respectively. The normalized difference in reflectivity ΔR in both

#145356 - $15.00 USD Received 4 Apr 2011; revised 20 May 2011; accepted 2 Jun 2011; published 19 Jul 2011

cases is around 30%. Thus, with proper modification, OCT system can be used to reject background signals that do not provide circular polarization dependent behavior and we can get signal with strength of around 30% of reflectivity. When combined with enhancement due to Plasmon resonance, we can achieve enhanced sensitivity in detection of nanoparticles.

Above results characterize the differential response from particles for pure LCP and RCP incident light. Form birefringence in biological tissues alters the polarization state of light and potentially introduces significant background. To assess the effect of polarization state change due to birefringence, we calculated normalized difference in reflectivity for various values of phase retardations. In this study, for both LCP and RCP, we obtained elliptical polarization state by applying the phase retardation in one of the linear orthogonal component. Field values were obtained for this altered polarized state. In Fig. 4, we have plotted normalized difference in the reflectivity for different values of phase retardation. Both LCP and RCP get converted into linearly polarized light at 90^0 phase retardation. Thus, at 90^0 phase retardation, we have same backscattered intensity leading to zero normalized difference in reflectivity. At 180^0 phase retardation, LCP converts into RCP and vice versa, so we should expect opposite sign in normalized difference in reflectivity.

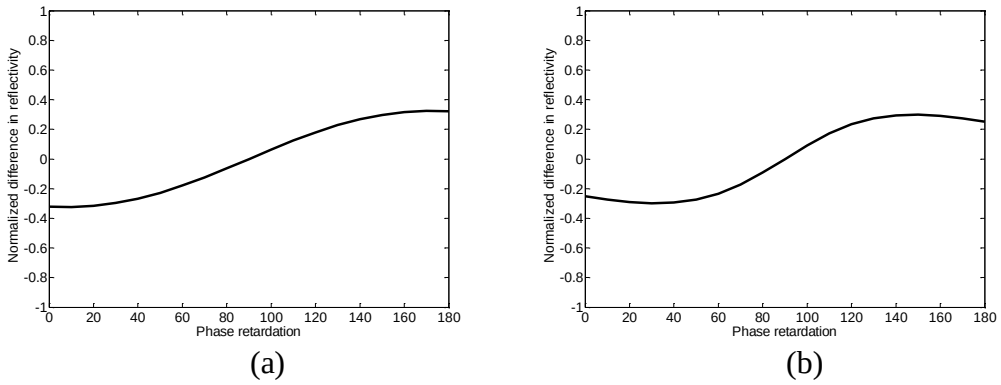

(a) (b)

Fig. 4. Effect of Phase retradation of media (Birefringence induced) on Normalized difference in reflectivity, Dimensions for (a): L = 70 nm, W = 30 nm, D = 68 nm, θ_r = 45°, Dimensions for (b): L = 175 nm, W = 30 nm, D = 81 nm, θ_r = 45°, NA = 0.35.

The real biological tissues introduce phase retardation values of around $0.6^0 / mm$ [20]. Thus, we can judge from Fig. 4 that such small phase change will not lead to significant change in the value of normalized difference in reflectivity.

In practice, it is difficult to fabricate structures with precise dielectric width. Therefore, it is important to assess the response for various values of dielectric layer width (D). Figure 5 displays the effect of dielectric layer width on ΔR . We notice that the changes in dielectric layer width do not have significant effect on ΔR .

#145356 - $15.00 USD Received 4 Apr 2011; revised 20 May 2011; accepted 2 Jun 2011; published 19 Jul 2011

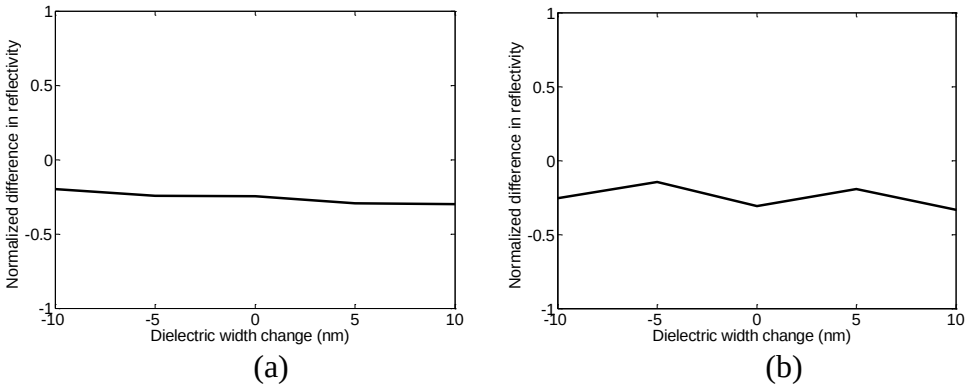

Fig. 5. Effect of dielectric layer width change on normalized difference in reflectivity (a): L = 70 nm, W = 30 nm, D = 68 nm, θ_r = 45°, Dimensions for (b): L = 175 nm, W = 30 nm, D = 81 nm, θ_r = 45°, NA = 0.35.

Above results demonstrate that bilayer chiral nanoparticles can provide tunable wavelength and polarization dependent response. For above dimensions, particle scatters RCP incident light predominantly as compared to the LCP incident light. It is possible to tune this behavior by changing θ_r . In this work, we have demonstrated the effect of θ_r on the polarization dependent behavior. In the Fig. 4, we have calculated CIDS of the structure for different values θ_r . For $\theta_r = 0^o$ and $\theta_r = 90^o$, the structure looks symmetrical to the incident light, and consequently it will not provide polarization dependent behavior. Other values of θ_r will make it chiral and provide the polarization dependent behavior. Varying θ_r from 45^o to 135^o changes the handness of the particle and reverses the polarization dependent behavior. We can confirm this from Fig. 6, as CIDS is the same but with opposite sign.

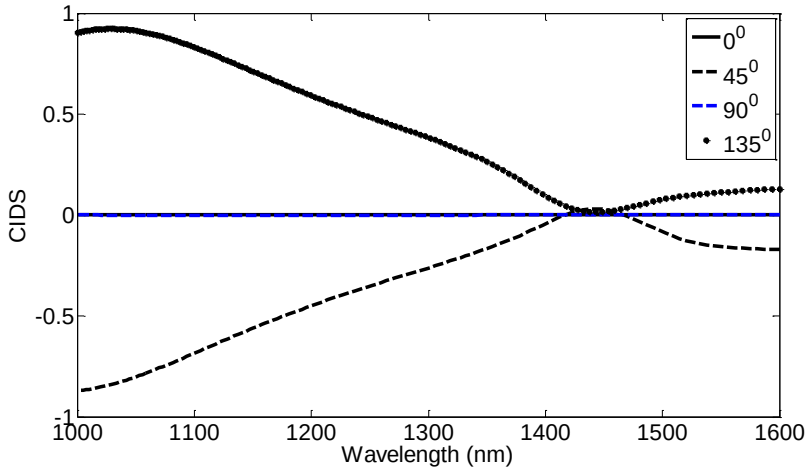

Fig. 6. Chirality tuning by changing θ_r CIDS obtained for θ_r = 0°, 45°, 90° and θ_r = 135°.

Next, we describe simple modifications to the conventional OCT system that can be used to detect the proposed chiral behavior. To implement our contrast mechanism, it is necessary to measure depth dependent reflectivity from the sample for LCP and RCP incident light. To achieve this measurement, the single-mode fiber based system with single detector can be modified as shown in the Fig. 7. In this setup, linearly polarized beam is obtained by using a

#145356 - $15.00 USD Received 4 Apr 2011; revised 20 May 2011; accepted 2 Jun 2011; published 19 Jul 2011

free space isolator. This linearly polarized light can be converted into circularly polarized beam by using a quarter wave plate (QWP). By adjusting optical axis of QWP1 at either 45^0 or -45^0 with respect to linearly polarized light, we can get LCP or RCP light.

As the back reflected light has both LCP and RCP components it is necessary to take two scans to extract the reflectivity. In one scan the reference arm signal is LCP and in the second scan it is RCP. This two scan mechanism will allow determination of depth dependent reflectivity with a single detector. QWP2 controls the polarization state of the light in reference arm. For one scan QWP2 is absent in the reference arm, in this case there will be flip in the polarization state due to reflection by mirror. In second scan, QWP2 is inserted into the reference arm. In this way we can switch between LCP and RCP signal from the reference arm. Using this simple modification, total of four scans and post processing allow us to determine differential reflectivity and achieve enhanced contrast.

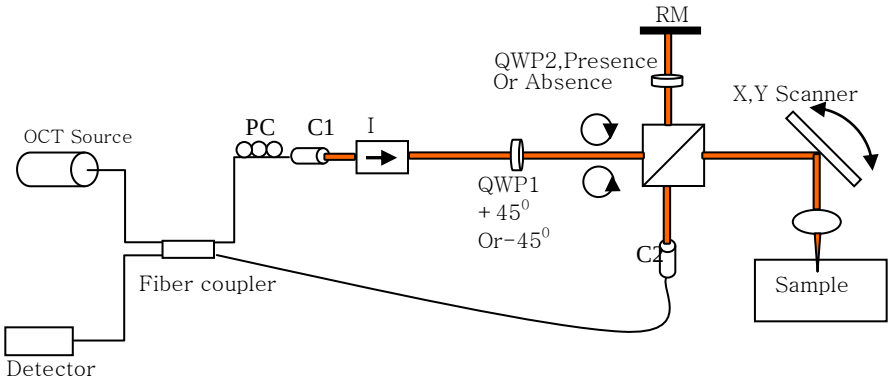

Fig. 7. Single detector Circular polarization sensitive OCT, PC: Manual fiber polarization controller, C1, C2: Fiber collimator, QWP1, QWP2: Quarter wave plates, RM: Reference mirror, I: Free space Isolator.

E-beam lithography based process can be used to fabricate such chiral nanoparticles. The current approach for fabrication that we are working on is based on a method used in [15]. In [15], authors had fabricated an array of mutually twisted double layer gammadion structure. To obtain the particles, few additional steps are necessary after coating silicon nitride on the first layer of gold nanorods. Photolithography process needs to be carried out to get island of particles. Again we can continue the process mentioned in [15] to pattern second layer of twisted gold nanorods. This will generate array of double layer structure. Next additional step is of processing with HF (hydrofluoric) acid that dissolves the silica layer [21]. This step will separate particles from the substrate layer. The overview of process is displayed in Fig. 8. Apart from E-beam lithography, we are also exploring possible chemical methods to fabricate such particles.

#145356 - $15.00 USD Received 4 Apr 2011; revised 20 May 2011; accepted 2 Jun 2011; published 19 Jul 2011

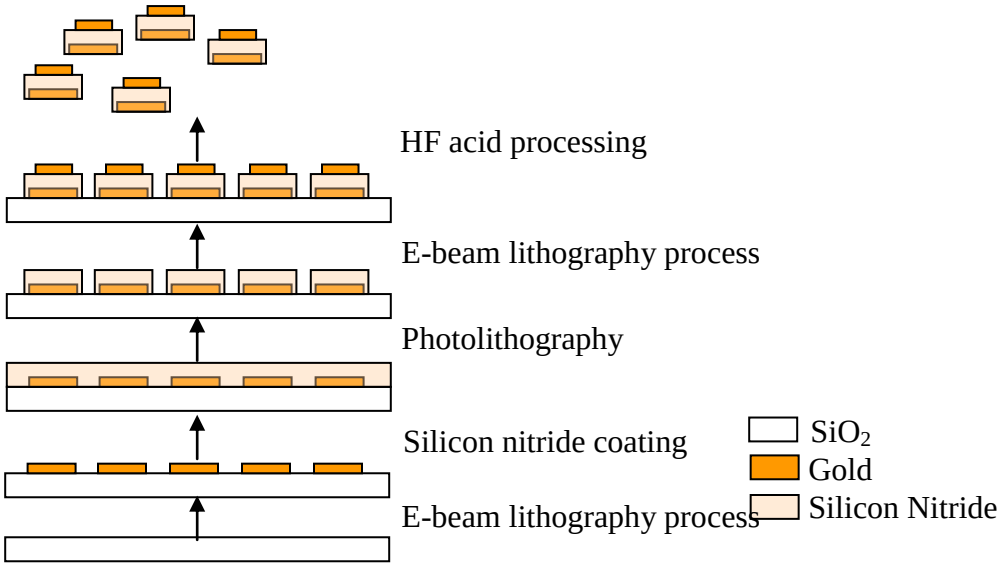

Fig. 8. Overview of nanoparticles fabrication method.

4. Conclusions

In summary, we have demonstrated the possibility of using a chiral metallic dual nanorod structure as polarization sensitive contrast agent. Using numerical simulations based on the FDTD method, it has been demonstrated that the structure has different scattering cross-sections for LCP and RCP incident light. Along with enhanced scattering due to Plasmon resonance, these particles can provide around 30% normalized difference in reflectivity with respect to the sense of circular polarization. We have described simple modifications in conventional OCT system to measure normalized difference in reflectivity. This circular polarization dependent behavior can provide an efficient method to achieve background signal rejection. These contrast agents should find wide use in biological applications that suffer from large background signal, such as deep tissue imaging.

Acknowledgments

We acknowledge financial support from A*STAR through SERC grant (No 102 152 0018). Kalpesh Mehta acknowledges the scholarship provided to him by NUS Graduate School of Integrative Sciences and Engineering. We acknowledge fruitful discussion and insight provided by Dr. Deng Jie from SERC-Nanofabrication and Characterization, IMRE for providing useful input on fabrication method. We also acknowledge Dr. Shalin Mehta, Optical Bioimaging lab, NUS for proof-reading our manuscript and providing useful suggestions.

#145356 - $15.00 USD Received 4 Apr 2011; revised 20 May 2011; accepted 2 Jun 2011; published 19 Jul 2011